

Raman spectroscopy of nanocrystalline and amorphous GaN

H. J. Trodahl, F. Budde, B. J. Ruck, S. Granville, A. Koo et al.

Citation: *J. Appl. Phys.* **97**, 084309 (2005); doi: 10.1063/1.1875743

View online: <http://dx.doi.org/10.1063/1.1875743>

View Table of Contents: <http://jap.aip.org/resource/1/JAPIAU/v97/i8>

Published by the [AIP Publishing LLC](#).

Additional information on J. Appl. Phys.

Journal Homepage: <http://jap.aip.org/>

Journal Information: http://jap.aip.org/about/about_the_journal

Top downloads: http://jap.aip.org/features/most_downloaded

Information for Authors: <http://jap.aip.org/authors>

ADVERTISEMENT



AIPAdvances

Now Indexed in
Thomson Reuters
Databases

Explore AIP's open access journal:

- Rapid publication
- Article-level metrics
- Post-publication rating and commenting

Raman spectroscopy of nanocrystalline and amorphous GaN

H. J. Trodahl,^{a)} F. Budde, B. J. Ruck, S. Granville, and A. Koo

MacDiarmid Institute for Advanced Materials and Nanotechnology, School of Chemical and Physical Sciences, Victoria University of Wellington, P.O. Box 600, Wellington, New Zealand

A. Bittar

Industrial Research Ltd., P.O. Box 31310, Lower Hutt, New Zealand

(Received 28 June 2004; accepted 10 January 2005; published online 5 April 2005)

We report Raman measurements on thin films of strongly disordered GaN and GaN:O prepared by ion-assisted deposition. The incident photon energies used in the experiments ranged from 1.95 to 3.8 eV, spanning the interband edge. Under subgap excitation the signal resembles the crystalline GaN vibrational density-of-modes, with significant broadening as expected for disordered material. There is a strong resonant behavior at the interband edge of the same mode for which a strong resonance is found in crystalline GaN, with a width suggesting that the entire vibrational branch contributes to the signal. Even nanocrystalline material is found to display Raman spectra characteristic of very short-range (<1 nm) translational symmetry, in agreement with x-ray diffraction evidence for the random stacking nature of the 3 nm diameter crystallites. The presence of oxygen at even 25 at. % has only a subtle effect on Raman spectra at the network vibrational frequencies below 800 cm^{-1} , but its presence is signaled by the appearance of an oxygen mode at 1000 cm^{-1} . An N_2 line at 2360 cm^{-1} correlates with a nitrogen excess introduced during growth. © 2005 American Institute of Physics. [DOI: 10.1063/1.1875743]

I. INTRODUCTION

Gallium nitride has been extensively studied over the past decade, work that is encouraged by its success as the material of choice for light emission in the blue-green region of the spectrum. One unexpected characteristic of the material is the insensitivity that it exhibits toward a high density of crystal defects, so that recently there have been observations of possibly useful optoelectronic behavior in polycrystalline material.^{1,2} In fact the tolerance of GaN to structural disorder has been cited as evidence that even its amorphous form (*a*-GaN) might have useful optoelectronic properties.^{3,4} These developments, along with the need to understand the damage and annealing behavior of ion implanted GaN,⁵ require the exploration of reliable structural characterization tools. Among these Raman spectroscopy is one of the most powerful, particularly for its ability to provide structural information at an in-plane resolution as high as $1\text{ }\mu\text{m}$. There are a number of reports in the literature about the Raman signals in disordered GaN, especially after ion implantation and during subsequent annealing. However, the structural inferences that can be drawn from Raman spectra are not as readily apparent as are, for example, those of ray diffraction (XRD), and with that in mind we report here an extensive study of the resonant Raman spectra on a variety of well characterized, strongly disordered GaN films prepared by ion-assisted deposition (IAD).

In the next section the IAD preparation procedure is briefly described, and the results of direct compositional and structural studies are reviewed. In Sec. III we discuss the Raman data and its interpretation in terms of the vibrational and electronic properties of the material. It will be seen that

there is information about the intermediate-range order that can be inferred from the data. Finally, in Sec. IV we summarize our conclusions.

II. EXPERIMENTAL DETAILS

A. Film preparation and characterization

The IAD films used in this work were prepared by exposing the substrates to a stream of Ga from a thermal source (either resistively- or electron-beam-heated) while simultaneously bathing it in energetic nitrogen ions from a Kaufmann source.⁶⁻⁹ They were grown to a thickness of typically 100–200 nm on Si, quartz, and glassy carbon substrates, and their compositions were determined by Rutherford backscattering spectroscopy (RBS) and nuclear reaction analysis.¹⁰ Stoichiometry is achieved only at high ion dose and energy, with 300–600 eV ions at a flux typically a few times that of the Ga atoms; lower ion energy or flux results in Ga-rich films. Films prepared with base pressures of less than 10^{-8} mb lead to near-stoichiometric material, with some excess N in the form of molecules.¹¹ Films have also been prepared with hydrogen by introducing mixed H_2 and N_2 gas into the ionization source, while up to 25 at. % oxygen and 7 at. % hydrogen is found in films prepared in the presence of water vapor at a pressure of a few times 10^{-6} mb.

Ga-edge extended ray absorption fine structure (EXAFS) data show that the Ga ions are nearly all fourfold coordinated, bonded to four N ions (a low density of which could be O) at the same distance as found in fully crystalline GaN (*x*-GaN).^{7,9} The second nearest neighbors appear in EXAFS only very much attenuated in comparison with *x*-GaN, in common with other tetrahedrally bonded amorphous III–V compounds or group IV elements.^{12,13} The spec-

^{a)}Electronic mail: joe.trodahl@vuw.ac.nz

tra can be fitted by 12 Ga second nearest neighbors, though disorder in the tetrahedral angles gives the second-neighbor distances a range which greatly reduces the second-neighbor feature. Thus our films are predominantly heteropolar bonded with a local tetrahedral configuration, and with defects consisting of O substituting for N and some level of molecular N₂.¹ In the following we refer to the films with 2% or less oxygen, and with up to 10% excess nitrogen residing in molecular form, as stoichiometric.

XRD and electron diffraction show amorphous patterns if 15 at.% or more oxygen is incorporated in the films, otherwise the films are nanocrystalline.¹⁴ Even in the nanocrystalline material (*x*-GaN) the widths of the XRD features are consistent with only very short-range order, extending to about 3 nm. Note that this XRD pattern relates almost entirely to the Ga–Ga radial distribution function and is determined largely by Ga layer spacing, so that this 3 nm range is the distance over which Ga planes show consistent spacing. It is thus not clear from these XRD results that the order corresponds to wurtzite or zinc blende structures, and in view of the limited energetic difference between the two forms of GaN, it is likely that the films have regions of randomly stacked planes of GaN tetrahedra. XRD patterns of the nanocrystalline films are well represented by a model of random stacked quasicrystallites.¹⁴

B. Raman spectroscopy

Raman spectroscopy was performed on a Jobin-Yvon LabRam HR spectrometer fitted with 2400 (UV-blue) and 600 (red) line per mm gratings. Excitation sources were a HeCd laser (325 nm), an Ar ion laser (458 and 514 nm), and a HeNe laser (633 nm). The spectra were taken at ambient temperature through a microscope, with a focus spot of 1–2 μm exposed to 1–5 mW. Care was taken to ensure that sample heating did not lead to any annealing development in the films, which has an onset of about 300° C,^{7,15} and the uniformity of Raman spectra across each film was carefully checked. All of the data we report here are from samples deposited on Si substrates, but the signals from samples deposited on other substrates were essentially identical.

Most of the films were transparent to visible light, so that the substrate signal appears in the raw spectra for all but 325 nm excitation. In particular the first order Si line at 521 cm^{-1} was stronger than the sample signal by typically two orders of magnitude; it often saturated the charge coupled device. That strong line could seldom be completely removed by subtraction, so there is often a gap at that frequency in the data displayed later. Furthermore, the GaN Raman spectra in even the thickest films were comparable in magnitude to the second-order Si signal from the substrate, which has in the past been mistaken for an *a*-GaN spectrum.¹⁶ In the present work we have subtracted the second order substrate signal.

An interpretation of resonance Raman on the films is aided by knowledge of their optical conductivity, which we have determined from reflectance-transmittance measurements using films on quartz substrates.

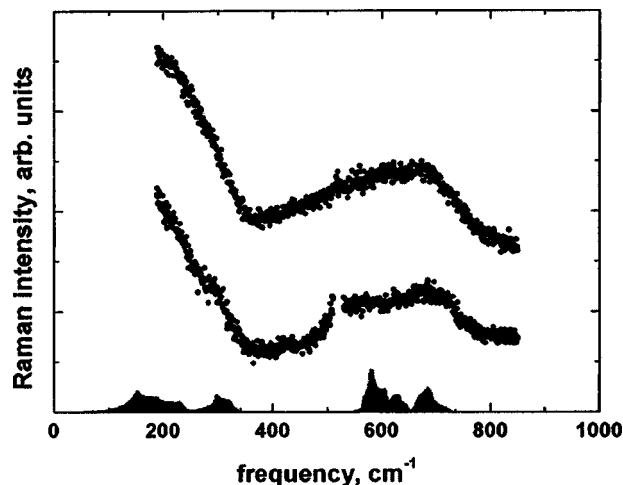


FIG. 1. Raman spectra collected with 514.5 nm excitation on a Ga-rich film (upper spectrum) and from a near-stoichiometric nanocrystalline film (lower spectrum). The calculated density of vibrational modes in *x*-GaN is shown in black at the base of the diagram.

III. RESULTS

We display first in Fig. 1 the Raman spectra of two films with differing Ga/N ratios, compared with the vibrational density of modes calculated for wurtzite GaN.¹⁷ There are two bands in the data, one above 400 cm^{-1} corresponding to the optic branches in *x*-GaN, and another below that frequency aligned with the acoustic band. The stoichiometric film shows weak structure in both bands, in good agreement with the main peaks in the GaN density of modes. The absence of narrow zone-center modes, or even the singularities in the computed density of modes, and their replacement with very much broadened features is in agreement with the lack of bonding order beyond a few nanometers. It is the long-range wave-like nature of the crystalline excitations that ultimately introduces the singularities, in association with stationary points in the phonon dispersion. It is interesting that the Ga-rich film shows broad vibrational excitations across the same bands as stoichiometric GaN, but without any structure within the two bands, and especially the lower frequency optic-band feature centered on about 550 cm^{-1} is lost. Furthermore, the Ga-rich film shows no evidence of the Si substrate spectrum, for this film is opaque owing to Ga-related midgap states. The transparent stoichiometric film has had the Si spectrum subtracted as mentioned earlier, though the subtraction is incomplete near the 521 cm^{-1} Si line.

A. Resonant Raman signatures of disorder

The dependence on excitation energy is shown for nanocrystalline GaN in Fig. 2. These spectra have been normalized by the integrated Si signal from a polished substrate, using the same collection geometry as for the films, and then corrected for the excitation frequency dependence of the Si signal.¹⁸ A further optical skin depth correction was required for green, blue, and UV excitations, based on the optical constants determined from reflection-transmission measurements; see Fig. 3. This skin depth correction was less than 50% except at 325 nm, where it was a factor of between 4

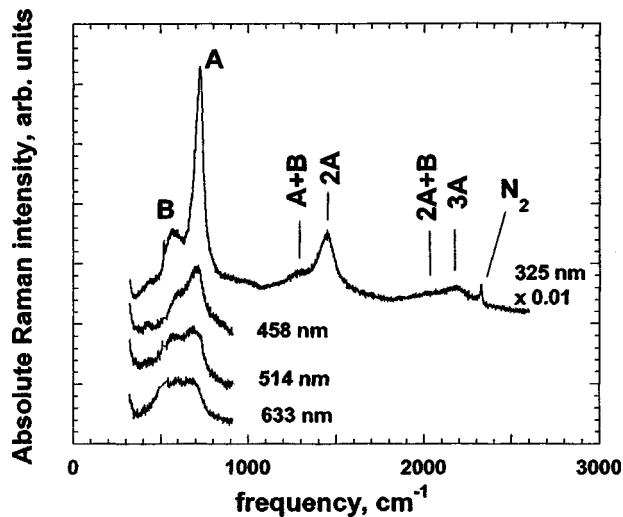


FIG. 2. Frequency dependence of the absolute Raman scattering cross section for a film with composition (Ga:N:O) of (47:51:2). Only the first order scattering is displayed for the visible excitation lines, and up to third order is shown for 325 nm excitation. Note that the acoustic branches are omitted in these spectra.

and 10. No corrections were made for the effect of multiple reflections or interference in the film, and that and uncertain geometric factors add to an uncertainty of about 50% in the comparability of the relative Raman cross sections. Nonetheless there are clear resonant enhancements seen in the data, for example in the increasing prominence of the features labeled “A” (730 cm^{-1}) and “B” (566 cm^{-1}), as the energy of the excitation photon rises. These two features, which have been reported previously in nanocrystalline GaN,¹⁹ span the frequencies at which there are clearly assigned zone-center modes in both wurtzite and cubic GaN.^{20,21} The 730 cm^{-1} line rises to completely dominate the spectrum at 325 nm (3.8 eV), exactly as is seen for the corresponding mode in GaN.^{22–24} Furthermore, this more strongly resonant feature can be followed easily to second and third order. There are shoulders on these higher order features as well, corresponding to combination modes A+B and 2A+B, but no features at overtones of B alone. The two resonant features are broad compared with their crystalline counterparts; as stated earlier they span lines appearing in cubic GaN and

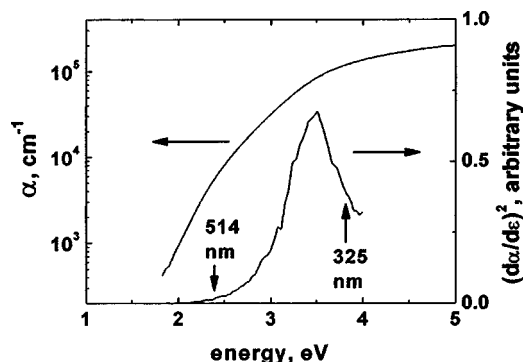


FIG. 3. Upper curve: the absorption coefficient for the film of Fig. 2, determined from reflection-transmission measurements. Lower curve: The square of the energy derivative of the absorption coefficient. The energies of two of the excitation sources are indicated by labeled arrows.

multiple peaks in wurtzite GaN. Such broad lines are characteristic of severely disordered materials, and we now demonstrate the use of the width of the 730 cm^{-1} line to estimate the range over which crystalline-like bonding order persists.

A broadening of Raman active lines in nanocrystalline materials results from the loss of well-defined phonon wave vectors.^{25,26} The termination of crystalline order at the diameter D leads to a range of effective wave vectors of order π/D associated with each phonon, so that phonons within π/D of the gamma point show some weight at the zone center, partially relaxing the wave vector selection rule. The observed Raman lines then broaden as dictated by the frequencies of these off-center phonons. The crystalline GaN optic branches that terminate near 730 cm^{-1} can be seen in normal-mode calculations to extend to a full-branch width of about 50 cm^{-1} .¹⁷ The full width at half maximum of the line in most of our spectra is in the range of 45–55 cm^{-1} , with the exception discussed later. Thus the entire branch has become Raman active, as for the other branches, but unlike the others this branch shows strong resonance at 325 nm. The result implies that the vibrational modes associated with the feature have very broad wave vector distributions, extending throughout the entire Brillouin zone, and in turn that full crystalline order extends to no more than a few lattice parameters. The apparent disagreement between the range of 3 nm found in XRD studies and the range of less than 1 nm from Raman spectroscopy is easily understood as arising from the random-stacked nature of the nanocrystals in the films, which introduce disorder at a scale much smaller than the quasicrystal dimensions.

It is important to note the relationship between the resonant enhancement of the 730 cm^{-1} line and the interband absorption edge in the films. The optical conductivity of the film corresponding to Fig. 2 is shown in Fig. 3. It can be seen that there is an increased absorption at much the same energy (3.4 eV) as in the crystalline material,^{27,28} though the edge is broadened by at least 100 meV, and there is substantial sub-band gap absorption. A simple deformation-potential resonant contribution to Raman scattering might be expected to vary as $|\partial_\chi/\partial_e|^2$ where ∂_χ and ∂_e are the material's susceptibility and photon energy, respectively.²⁹ In these films the real part of the conductivity carries the strongest energy dependence, and the square of its derivative is shown in the insert of Fig. 3. It can be seen that the 730 cm^{-1} vibrational band in nx -GaN is especially resonant at the interband edge, exactly as is its corresponding zone-center phonon in x -GaN.^{27,28} The excitation at 325 nm (3.8 eV) lies above the energy of strongest expected resonance; a slightly lower energy of 3.5 eV (353 nm) would be in full resonance.

B. Nanocrystalline-to-amorphous films

Figure 4 compares UV-excited Raman data for four films, all with close to 1:1 Ga:N ratios but with varying concentrations of oxygen and hydrogen. The two films with little oxygen have very similar spectra, and both are well represented by the data of Fig. 2. In contrast the film with the most oxygen shows a stronger and broader signal. The enhanced strength results from this film being more closely on

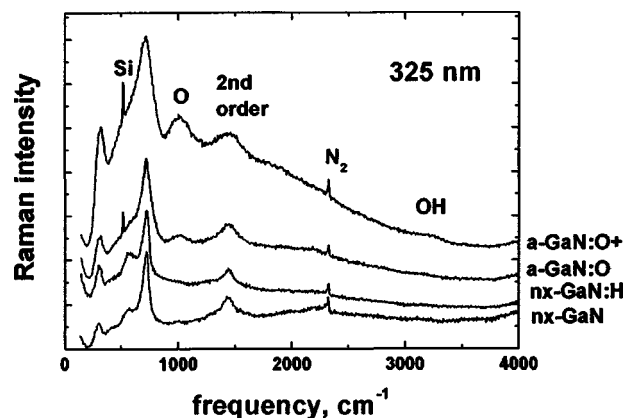


FIG. 4. UV-excited Raman spectroscopy of four GaN films with N:Ga ratios in the range of 1.0–1.2. From the top the films have (O:H) concentrations in atomic percent of (23;7), (12;3), (1;3), and (1;0). The top, heavily oxygenated, film was amorphous, the second was mixed amorphous/nanocrystalline, and the lowest two were nanocrystalline. The lowest spectrum was on a film that was 10% nitrogen rich (N:Ga of 1.2), a situation that is signaled by the strongest molecular nitrogen feature.

resonance, for it displays both an increased band gap and a sharper absorption edge than the oxygen-free films. However, it is also noticed that the narrow 730 cm^{-1} line is not prominent in this spectrum, so that the spectrum resembles the broad density-of-modes pattern found in nonresonant visible-light excitation (Fig. 1). The film with intermediate oxygen concentration, in contrast, shows elements of both the density-of-modes pattern and the resonant signal of the oxygen-free films. XRD on this film also reveals a nanocrystalline-amorphous mixture.¹⁴

In addition to its influence on the Raman spectrum of the predominantly GaN network, the presence of oxygen is signaled by a very broad oxygen vibration centered on 1000 cm^{-1} . We are as yet unable to associate the feature with any specific bonding configuration, and its width suggests that it arises from oxygen ions bonded into a variety of positions. Its strength can be seen to scale approximately as the oxygen concentration, though resonance effects are also likely to affect the Raman scattering from the oxygen vibrational modes.

The rather narrow line at about 2360 cm^{-1} seen in all of the UV spectra of Fig. 4 and to expanded scale in Fig. 5 corresponds to the stretching mode in molecular nitrogen, and confirms nitrogen-edge x-ray absorption evidence for the presence of molecular nitrogen in the films.¹¹ Some of the raw spectra on these films show small residual narrow N_2 and O_2 peaks arising from the air above the film, but their strength has been limited by exploiting the confocal nature of the Raman microscope. The atmospheric O_2 line at 1556 cm^{-1} was also monitored to track and correct for the atmospheric N_2 signal. Thus the strength of the remaining N_2 signal provides a measure of the two-dimensional density of molecular nitrogen within the Raman probed depth. The strongest integrated N_2 line in Figs. 4 and 5 is in a film with 10% excess nitrogen, followed closely by the most heavily oxygenated film. We have earlier noted that much of the oxygen appears to substitute for nitrogen, releasing molecular nitrogen in the process.¹¹ The width of the buried N_2

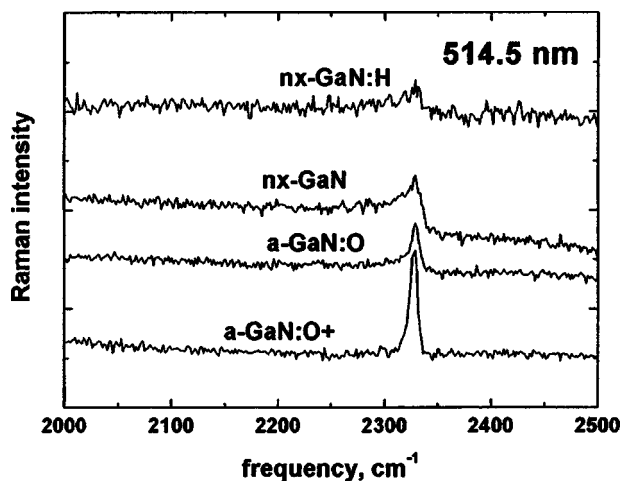


FIG. 5. Expanded 325 nm spectra in the molecular nitrogen region for the four films of Fig. 4.

signal, at 30 cm^{-1} only about 1% of the central frequency, is nonetheless much larger than the free air mode, suggesting a weak interaction between the buried molecular nitrogen and the GaN host.

Finally, Fig. 6 shows an expanded view of a hydrogen line at 3260 cm^{-1} . The frequency suggests either N-H^{30} or O-H^{31} bond-stretching vibrations. However, the mode appears here only in films containing O as well as H; it is not found in the GaN film containing solely H. It is clearly an OH line, and thus there is no evidence of N-H bonds in these data.

IV. CONCLUSIONS

The Raman spectra of strongly disordered GaN have been measured with excitation energies across the visible-near UV spectral region. The films were prepared by ion-assisted deposition, both as stoichiometric GaN and with up to 25 at.% oxygen. Oxygen-free films consist of random-stacked GaN nanocrystals and display Raman spectra as would be expected for noncrystalline material, resembling the density of vibrational modes of x -GaN. There is clear evidence of an UV resonance in one vibrational branch, the

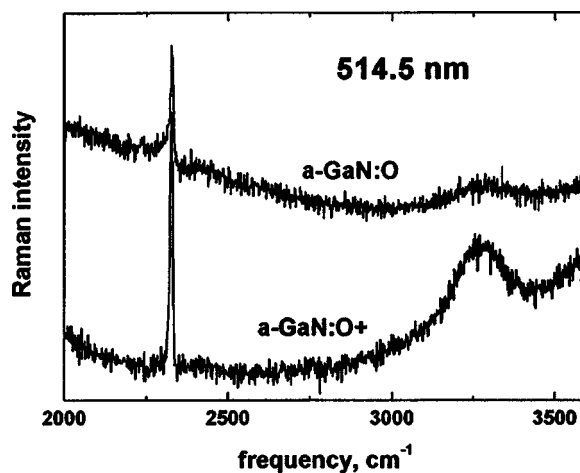


FIG. 6. 514.5 nm-excited Raman spectra of the two oxygenated films, showing both the molecular nitrogen and the OH vibrational modes.

same branch for which the zone-center vibration is strongly resonant in fully crystalline GaN, and the width of the feature in our spectra is in agreement with the width of the entire phonon branch in wurtzite GaN. The full body of data indicate that the films are formed of a very strongly disordered but heteropolar bonded covalent network, but with crystalline order extending over no more than a few lattice constants, rather smaller than the 3 nm crystallite diameters determined by XRD patterns. The apparent disagreement is resolved by noting that the zone-center selection rule operating in Raman scattering is sensitive to the loss of translational symmetry associated with random stacking, while in contrast the widths of XRD features depend primarily on a coherent separation of Ga planes and are thus largely unaffected by random stacking.

The introduction of oxygen at 15–25 at. % leads to the growth of amorphous films, but apart from a reduction of structure within the optic branch the Raman spectra are very similar to the density-of-mode patterns in nanocrystalline films. Thus the vibrational spectra of these films are also characteristic of a predominance of tetrahedral bonded Ga and N ions, a conclusion that follows also from previously published EXAFS data. It is not easy to detect the presence of oxygen by examining the network vibrational spectrum alone, but we find a clear oxygen-related feature centered on 1000 cm^{-1} .

The IAD method employed for oxygen-bearing film growth has led also to the incorporation of hydrogen, and the films then show an OH vibration at 3260 cm^{-1} . No hydrogen line has been observed in oxygen-free films containing hydrogen. Finally, there is evidence of molecular nitrogen in essentially all of our films, at a level consistent with the typically 5%–10% excess nitrogen detected by RBS.

ACKNOWLEDGMENTS

This work was supported by the New Zealand Foundation for Research Science and Technology under the New Economy Research Fund and by a Postdoctoral Fellowship (B.J.R.) and a Ph.D. Fellowship (A.K.). The work of the MacDiarmid Institute is supported by a New Zealand Centre of Research Excellence award.

¹K. Yamada, H. Asahi, H. Tambo, Y. Imanishi, K. Ohnishi, and K. Asami, *Appl. Phys. Lett.* **78**, 2849 (2001).

²D. P. Bour, N. M. Nickel, C. G. V. de Walle, M. S. Keissl, B. S. Krusor, P.

Mei, and N. M. Johnson, *Appl. Phys. Lett.* **76**, 2182 (2000).

³P. Stumm and D. A. Drabold, *Phys. Rev. Lett.* **79**, 677 (1997).

⁴H. Chen, K. Chen, D. A. Drabold, and M. E. Kordesch, *Appl. Phys. Lett.* **77**, 1117 (2000).

⁵M. Katsikini, K. Papagelis, E. C. Paloura, and S. Ves, *J. Appl. Phys.* **94**, 4389 (2003).

⁶A. Bittar, H. J. Trodahl, N. T. Kemp, and A. Markwitz, *Appl. Phys. Lett.* **78**, 619 (2001).

⁷U. D. Lanke *et al.*, *Mater. Res. Soc. Symp. Proc.* **693**, 347 (2002).

⁸A. Koo, U. D. Lanke, B. J. Ruck, S. Brown, R. Reeves, A. Bittar, and H. J. Trodahl, *Mater. Res. Soc. Symp. Proc.* **693**, 621 (2002).

⁹A. Koo *et al.*, *Proceedings of the 16th Conference on the Physics of Semiconductors*, edited by A. R. Long and J. H. Davies (Institute of Physics Publishing, Bristol, 2003).

¹⁰V. John Kennedy, A. Markwitz, U. D. Lanke, A. McIvor, H. J. Trodahl, and A. Bittar, *Nucl. Instrum. Methods Phys. Res. B* **190**, 620 (2002).

¹¹B. J. Ruck *et al.*, *Phys. Rev. B* **70**, 235202 (2004).

¹²C. J. Glover, M. C. Ridgway, K. M. Yu, G. J. Foran, T. W. Lee, Y. Moon, and E. Yoon, *Appl. Phys. Lett.* **74**, 1713 (1999).

¹³G. de M. Azevedo, M. C. Ridgway, K. M. Yu, C. J. Glover, and G. J. Foran, *Nucl. Instrum. Methods* **190**, 851 (2002).

¹⁴F. Budde *et al.*, e-print cond-mat/0407659.

¹⁵C. E. A. Grigorescu *et al.*, *IEEE Proceedings of the International Symposium on Photonic Crystals*, edited by M. Marciniak, Warsaw July 2003, p. 337.

¹⁶Y. Kang and D. C. Ingram, *J. Appl. Phys.* **93**, 3954 (2003).

¹⁷C. Bungaro, K. Rapcewicz, and J. Bernholc, *Phys. Rev. B* **61**, 6720 (2000).

¹⁸A. Compaan and H. J. Trodahl, *Phys. Rev. B* **29**, 793 (1984).

¹⁹M. Kuball, H. Mokhtari, D. Chems, J. Liu, and D. Westwood, *Jpn. J. Appl. Phys.*, Part 1 **39**, L4753 (2000).

²⁰T. Azuhata, T. Sota, K. Suzuki, and S. Nakamura, *J. Phys.: Condens. Matter* **7**, L129 (1995).

²¹H. Siegle, L. Eckey, A. Hoffmann, C. Thomsen, B. K. Meyer, D. Schikora, M. Hankeln, and K. Lischka, *Solid State Commun.* **96**, 943 (1995).

²²V. Lemos, C. A. Arguello, and R. C. C. Leite, *Solid State Commun.* **11**, 1352 (1972).

²³D. Behr, J. Wagner, J. Schneider, H. Amano, and I. Akasaki, *Appl. Phys. Lett.* **68**, 2404 (1996).

²⁴A. Kaschner, A. Hoffmann, and C. Thomsen, *Phys. Rev. B* **64**, 165314 (2001).

²⁵I. H. Campbell and P. M. Fouchet, *Solid State Commun.* **58**, 739 (1986).

²⁶G. V. M. Williams, A. Bittar, and H. J. Trodahl, *J. Appl. Phys.* **67**, 1874 (1990).

²⁷S. Logothetidis, J. Petalas, M. Cardona, and T. D. Moustakas, *Phys. Rev. B* **50**, 18017 (1994).

²⁸J. Petalas, S. Logothetidis, S. Bouladakis, M. Alouani, and J. M. Wills, *Phys. Rev. B* **52**, 8082 (1995).

²⁹M. Cardona, in *Light Scattering in Solids II*, edited by M. Cardona and G. Guntherodt (Springer, Berlin, 1982).

³⁰C. H. Seager, S. M. Myers, G. A. Etersson, J. Han, and T. Headly, *J. Appl. Phys.* **85**, 2568 (1999).

³¹B. Szymanik, R. G. Buckley, H. J. Trodahl, and R. L. Davis, *Solid State Ionics* **109**, 223 (1998).